Am J Cancer Res 2019;9(10):2216-2232
www.ajcr.us /ISSN:2156-6976/ajcr0102147

Original Article

LY2228820 induces synergistic anti-cancer effects with anti-microtubule chemotherapeutic agents independent of P-glycoprotein in multidrug resistant cancer cells

Ronggao Chen[1,2*], Yiting Qiao[1,2*], Wendi Hu[1,2], Qiyang Cheng[1,2], Haiyang Xie[1,2,3,4,5], Lin Zhou[1,2,3,4,5], Xiao Xu[1,2,3,4,5], Shusen Zheng[1,2,3,4,5], Donghai Jiang[1,2,3,4,5]

[1]Department of Surgery, Division of Hepatobiliary and Pancreatic Surgery, First Affiliated Hospital, School of Medicine, Zhejiang University, Hangzhou 310000, Zhejiang Province, China; [2]NHFPC Key Laboratory of Combined Multi-Organ Transplantation, Hangzhou 310000, Zhejiang Province, China; [3]Key Laboratory of The Diagnosis and Treatment of Organ Transplantation, CAMS, China; [4]Key Laboratory of Organ Transplantation, Hangzhou 310003, Zhejiang Province, China; [5]Collaborative Innovation Center for Diagnosis Treatment of Infectious Diseases, Hangzhou 310000, Zhejiang Province, China. [*]Equal contributors.

Received September 10, 2019; Accepted September 20, 2019; Epub October 1, 2019; Published October 15, 2019

Abstract: Side-effects and resistance substantially limit the efficacy of chemotherapy. One possible solution to this persistent problem would be co-administration of targeted therapy and chemotherapy to achieve synergistic anti-cancer effects without extra toxicity. Here, we reported that LY2228820, a selective inhibitor of p38-MAPK signaling pathway, could induce synergistic anti-cancer effects with anti-microtubule (AMT) chemotherapy both *in vitro and in vivo*. In drug-resistant cancer cells, treatment with either LY2228820 or AMT drug alone was compatible with viability, while co-administration of both led to dramatic cytotoxicity, G2/M arrest and apoptosis. Moreover, co-treatment with LY2228820 notably improved the effectiveness of paclitaxel without exhibiting adverse effects *in vivo*. Mechanistic studies showed that LY2228820 sensitized cancer cells to AMT agents independent of P-gp. LY2228820 did not influence either the expression or the function of P-gp. Instead, it could inhibit p38-HSP27 signaling axis by down-regulating p-HSP27. Furthermore, LY2228820 blocked the p-HSP27 mediated protective response against AMT drugs in tumor cells, resulting in mitochondrial instability and the activation of mitochondrial death pathways. This P-gp-independent regime containing LY2228820 and AMT agents could produce synergistic anti-cancer effects without extra systematic toxicity. Our study offers a novel strategy for improving the therapeutic efficacy of AMT drugs by achieving a better balance between efficacy and toxicity. This new combination regime could be advantageous in patients who show little response to the maximal dosage of AMT chemotherapy, as well as those unable to tolerate the systematic toxicity of these agents in clinic.

Keywords: Synergistic anti-cancer effects, LY2228820, anti-microtubule agents, P-gp, p-HSP27, mitochondrial death

Introduction

Currently, chemotherapy can be classified into two categories: conventional chemotherapy with cytotoxic agents which suppress the fundamental biological process of rapidly dividing cells, and targeted therapy aimed at blocking the hyper-activated signaling pathways which are critical for cancer cells yet spare normal cells [1]. Both have unique advantages and disadvantages. For instance, conventional chemotherapy has a wider response among various cancer types, while the efficacy of targeted therapy varies greatly among cancer types due to its high dependence on the presence of proper therapeutic targets [2]. Besides, conventional chemotherapy often exhibits more severe systematic toxicity to organs with high cell turnover such as the bone marrow and digestive tract, while targeted therapy maintains better tolerance among patients [3, 4]. Moreover, cancer cells also utilize different strategies to develop resistance against these two therapeutic categories. For conventional chemotherapy, reducing drug influx or enhancing drug efflux are the most common mechanisms of drug resistance, while the alteration of signaling networks via bypassing therapeutic targets

often occurs in cells resistant to targeted therapy [5].

Consequently, it is reasonable to combine conventional and targeted chemotherapies together to complement each other. Generally, the effects of combing different treatments can either be antagonistic, additive or synergistic. It is worth noting that systematic toxicity could accumulate when two toxic drugs are used in combination [6]. Therefore, the ideal form of combination therapy should be able to cause significant injury to tumor cells with a low-toxic dosage of a cytotoxic agent in combination with a non-toxic targeted therapy. Therefore, individual components alone has little influence on either cancer cells or healthy tissues, but specific and remarkable injury to malignant tissues results from their combination, thus greatly improving the therapeutic efficacy as well as the quality of life for patients. For example, thioridazine, an established antipsychotic agent, sensitizes glioblastoma cells to temozolomide by blocking autophagy, thus significantly increasing the survival in drug-resistant glioblastoma, while avoiding the severe systematic toxicity commonly seen in animals treated with a higher dose of temozolomide alone [7].

The reported study is another typical example of synergistic anti-cancer chemotherapies. Here, we studied two anti-microtubule (AMT) agents, paclitaxel and vinorelbine, both of which can interfere with the tubulin dynamics and interrupt proper chromosome segregation, thus causing mitotic catastrophe and cell death. Their side-effects include digestive tract symptoms (nausea, vomiting and diarrhea), skin symptoms (pale skin and hair loss), peripheral neurotoxicity (joint or muscle pain) and even seizures [8]. These side effects limit the maximal dosage in clinic and increase the possibility of treatment interruptions, allowing a fraction of cancer cells to survive and develop resistance, thus leading to relapse. One possible solution to this long-standing problem is the construction of a balance between satisfactory therapeutic efficacy and tolerable systematic toxicity, by adding targeted therapy with relatively less systematic toxicity to reduce the dosage of cytotoxic AMT agents. Therefore, many efforts have been devoted to seeking a proper targeted therapeutic approach to sensitize cancer cells to these classic cytotoxic chemotherapies and to improve their therapeutic window for a better safety profile.

From a large-scale screening of small molecular compounds (> 1800) with potential antitumor activity, we identified that LY2228820, a P38/MAPK inhibitor with a good safety profile in phase 1/2 clinical trial, could achieve synergistic anti-cancer effects in combination with low doses of paclitaxel or vinorelbine in cancer cells both *in vitro* and *in vivo*. Moreover, mechanistic studies showed that such synergy was mediated by the suppression of HSP27 phosphorylation (ser78) rather than the blockage of P-gp activity. Therefore, the systematic toxicity of paxlitaxel or vinorelbine at high doses could be avoided by such synergistic anti-cancer therapies.

Materials and methods

Cell culture and mice

BCap37 was obtained from Prof. Weimin Fan (The Medical University of South Carolina) in 2010. Bads-200 and Bats-72, two multidrug-resistant (MDR) cell lines, were established from BCap37 as described previously [9]. HCC-LM3 was purchased from China Center for Type Culture Collection (CCTCC) in 2014. BCap37, Bads-200 and Bats-72 were maintained in RPMI 1640 medium supplemented with 10% fetal bovine serum (FBS), whereas Bads-200 was cultured with additional 200 nM paclitaxel. HCC-LM3 was maintained in minimum essential medium with 10% FBS. Cells were incubated at 37°C with 5% CO_2. All cell lines were tested negative for mycoplasma. 4-5-week-old female athymic nude (*nu/nu*) mice were purchased from the Animal Facility of Zhejiang University. All animals care and experiments were conducted according to the Guidelines of Zhejiang University Animal Care Committee.

Drugs and treatments

Paclitaxel (injection, 6 mg/mL) was purchased from Mead Johnson Co. (Princeton, NJ, USA). LY2228820 (50 mg) was purchased from Selleckchem (Houston, TX, USA). Cells were evenly seeded into various plates or dishes in drug-free medium for 24 h, and then treated with chemotherapeutic agents with or without the co-administration of LY2228820.

MTT assay

Cells were harvested and resuspended to a final concentration of 10^4 cells/mL. Aliquots

of the cell suspension were evenly distributed into 96-well tissue culture plates. After one night of incubation, the designated wells were treated with drug regimes. Four hours prior to the end of treatment, MTT solution was added. The medium containing MTT was replaced with 150 μL of DMSO in each well to dissolve the formazan crystals after 4 h-incubation. The absorbance at 570 nm in individual wells was determined using a microplate spectrometer (Bio-Rad, Sunnyvale, CA).

Colony-forming assay

Bads-200 cells were seeded into 6-well plates at a density of 500 cells/well and were maintained with different regimens of drugs for 12 days. The cell clones were stained with Giemsa.

Analysis of cell cycle

Cell cycle distribution was determined by flow cytometric analysis. Briefly, after drug treatment for 72 h, both detached and attached cells were harvested and washed twice with PBS, followed by fixation in 75% ethanol diluted in PBS. Cells were then incubated in PBS containing 100 μL/mL RNase and 40 μL/mL propidium iodide (PI) at room temperature for 0.5 h before flow cytometric analysis. Cell cycle distribution and DNA content were determined using Coulter Epics V instrument (Beckman Coulter, CA).

Analysis of apoptosis

Annexin V/PI apoptosis detection kit (Beyotime, Haimen, China) was used to detect cell apoptosis according to the manufacturer's instructions. Briefly, cells were harvested and washed twice with PBS after treatment for 72 h. Then the cells were suspended with 400 μL of binding buffer, 5 μL of Annexin V conjugated with fluorescein isothiocyanate (FITC) and 5 μL of PI solution. After incubating for 15 min at room temperature in the dark, the percentage of apoptotic cells was determined by flow cytometry.

Evaluation of therapeutic efficacy in vivo

Bats-72 cells (1 × 10^6 cells in 0.1 mL PBS) were implanted into the right flanks of the homozygous nude athymic mice (female, 5-6 weeks old). Four days after implantation, mice were randomly divided into 4 groups and treated with different regimens: (i) vehicle; (ii) LY2228820 alone at 20 mg/kg, i.v.; (iii) paclitaxel alone at 15 mg/kg, i.v.; (iv) combination of LY2228820 and paclitaxel, i.v.. The same treatment regimens were repeated every 3 days for a total of 5 cycles. Two perpendicular diameters (width and length) of the tumors as well as the body weight of mice were measured every 3 days until the animals were euthanized. After the animals were sacrificed, the tumor tissues were resected and weighted. Further, livers, kidneys and blood samples were examined. Serum alanine aminotransferase (ALT), aspartate aminotransferase (AST) and creatinine levels were measured using a Hitachi 7600 automatic analyzer (Hitachi, Tokyo, Japan). The inhibition rate of tumor growth (IR) was calculated according to the following formula: IR = 100% × (mean tumor weight of control group mean tumor weight of experimental group)/mean tumor weight of control group.

Rhodamine 123 efflux assay

Bads-200 cells were incubated with PBS, LY2228820 or verapamil for 3 h. 5 μM Rhodamine 123 (Meilunbio, Dalian, China) was then added in each group. The cells were incubated for additional 0.5 h. Afterwards, the cells were washed with ice-cold PBS, trypsinized and resuspended in 300 μL PBS. Intracellular Rhodamine 123 fluorescence intensity was determined with Coulter Epics V instrument (Beckman Coulter, CA).

P-glycoprotein ATPase activity assay

The effect of LY2228820 on the ATPase activity of P-glycoprotein was measured by P-gp-Glo™ Assay Systems (Promega, Madison, WI) according to the protocol provided by the manufacturer [10].

Mitochondrial membrane potential (MMP)

MMP was determined using a JC-1 mitochondrial membrane potential assay kit (Beyotime biotechnology, Hainan, China). Cells were collected, resuspended in PBS, and subsequently incubated with JC-1 for 30 min at 37°C in the dark. After incubation, the cells were washed and analyzed by flow cytometry.

Isolation of mitochondria and cytoplasm

The cell mitochondria isolation kit (Beyotime biotechnology, Hainan, China) was utilized to obtain cytosolic and mitochondrial protein frac-

tions. Cells were collected and incubated with mitochondria isolation reagent for 15 min in ice, then homogenized with glass homogenizer for 15-20 times. After centrifugation for 10 min (700 g, 4°C), the supernatant was isolated and centrifuged again for 30 min (10000 g, 4°C). Precipitate was mitochondrial fraction and supernatant was centrifuged for 10 min (12000 g, 4°C) to collect cytosolic fraction.

siRNA transfection

Cells were transfected with HSP27 siRNA (RiboBio, Guangzhou, China) using Lipofectamine 2000 (Invitrogen, USA) according to the manufacturer's protocol. The siRNA sequence for HSP27 was GCTGCAAAATCCGATGAGA.

Western blot analysis and antibodies

Cells were collected for western blot analysis after different treatments. The detailed procedure has been described previously [9]. The antibodies were listed as follows: β-actin (sc-47778) was from Santa Cruz Biotechnology, Inc. (Santa Cruz, CA, USA); cleaved caspase-3 (#9661), cleaved PARP (#5625), Cyclin B1 (#41-35), Cdc2 (#9116), P-gp (#13342), p-MKK3/6 (#12280), p-P38 (#4511), P38 (#8690), p-MK2 (#3041), p-HSP27 (#2405), HSP27 (#95357), Cytochrome C (#11940), β-tubulin (#2128) and COX-IV (#4850) were from Cell Signaling Technology, Inc. (Danvers, MA, USA); goat anti-rabbit and goat anti-mouse IgG peroxidase-conjugated secondary antibodies (31460 and 31-430) were purchased from Thermo-Pierce (Rockford, IL, USA).

Statistical analysis

Data are presented as mean ± standard error of three independent experiments. Two-sided Student's t-test was used to determine the statistical difference between various experimental and control groups. Statistical analysis of the data presented was performed by SPSS version 22.0 (SPSS, Chicago, IL, USA).

Results

LY2228820 induces synergistic effect with AMT agents in MDR breast cancer cells

First, the appropriate concentration of LY2228820 for the combination therapy was determined by MTT assay. As shown in **Figure 1A**, LY2228820 exerted little cytotoxicity from 0 to 2 μM, and hence 2 μM LY2228820 was chosen as the safe dosage for the co-administration with various chemotherapeutic agents. As shown in **Figure 1B**, **1C**, LY2228820 remarkably enhanced the cytotoxicity of paclitaxel in a MDR cell line Bads-200, and the IC50 values decreased from 1501 nM to 420.7 nM ($P < 0.001$). Besides, LY2228820 could also significantly sensitize Bads-200 to vinorelbine (**Figure 1D**). However, the co-treatment of LY2228820 had little influence on the drug sensitivity of doxorubicin and mitomycin in Bads-200 (**Figure 1E**, **1F**). The results obtained in Bats-72, another MDR cell line, were consistent with those obtained in Bads-200 (**Table 1**).

As depicted in **Figure 1G**, the overall cell morphology was normal in CTL and monotherapy groups of both paclitaxel/vinorelbine and LY2228820, and whereas their co-treatment induced abnormal morphology, including suspending cells, cytoplasm blebs and apoptotic bodies. In addition, colony-forming assay showed that while the number and size of colonies were comparable between CTL and monotherapy groups, almost no visible colonies were formed in the co-treatment group (**Figure 1H**). In a word, LY2228820 induces synergistic effect with AMT agents in MDR breast cancer cells.

LY2228820 enhances G2/M arrest and apoptosis induced by AMT agents

AMT agents exert cytotoxic effects by inducing G2/M arrest via stabilizing microtubules, which leads to apoptosis. As shown in **Figure 2A**, compared with the treatments of 500 nM paclitaxel and vinorelbine alone, their co-administration with 2 μM LY2228820 significantly increased the percentage of cells at G2-M phase, from 19.97% to 78.4% ($P < 0.001$) and 23.32% to 81.04% ($P < 0.001$), respectively. Similar results were obtained in Annexin V/propidium iodide apoptosis assay. As shown in **Figure 2B**, the co-treatment of LY2228820 significantly elevated the population of apoptotic cells compared to the groups treated with paclitaxel or vinorelbine alone ($P < 0.001$, 21.57% versus 6.23%, 19.63% versus 5.90%). A monotherapy of 2000 nM paclitaxel (PTX!) or 5000 nM vinorelbine (VB!) was required to

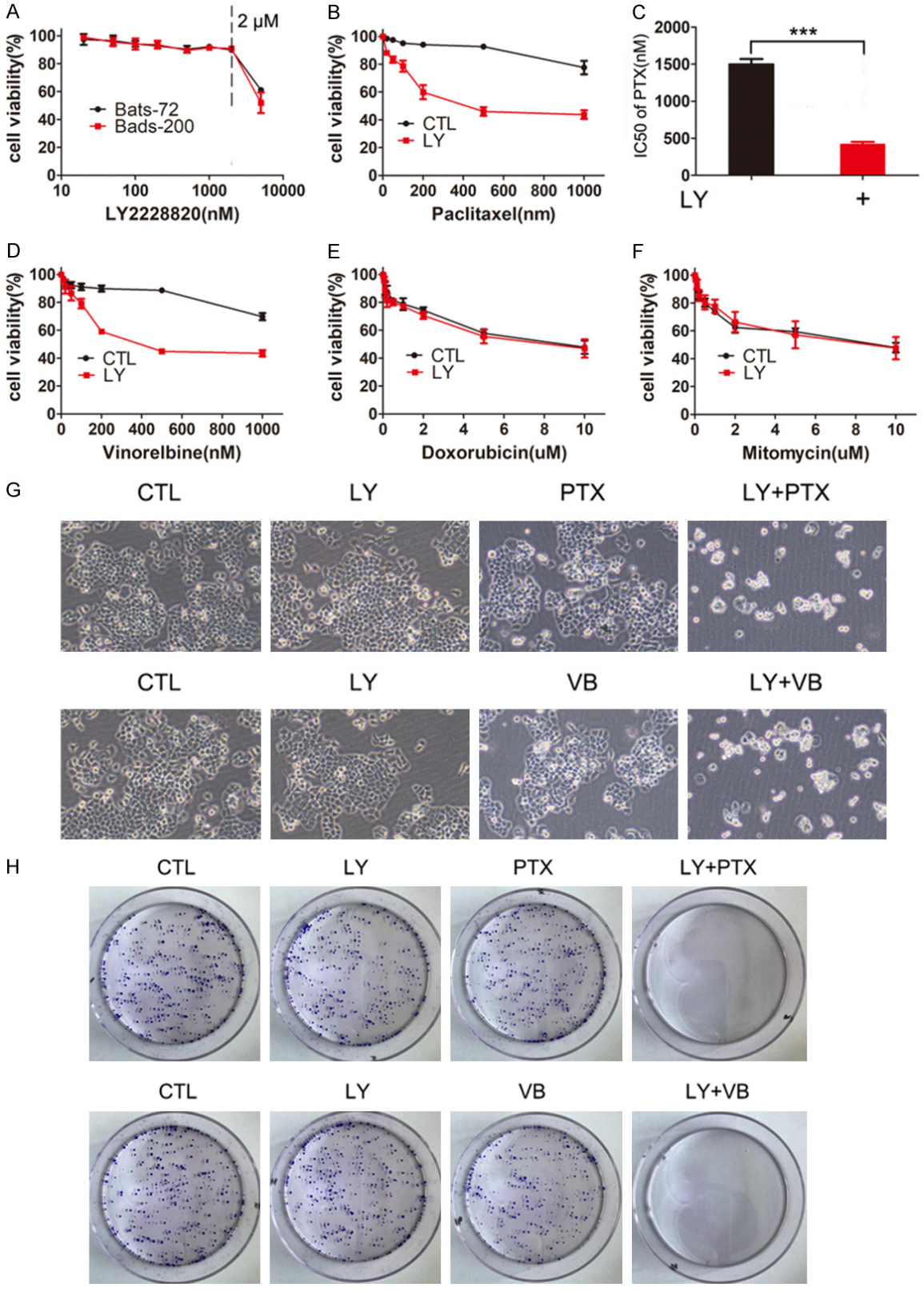

Figure 1. LY2228820 induces synergistic effect with AMT agents. A. Bads-200 and Bats-72 were incubated with increasing doses of LY2228820 alone for 72 h. B-F. Bads-200 was exposed to a series of concentrations of paclitaxel, vinorelbine, doxorubicin or mitomycin respectively with or without the combination of 2 μM LY2228820 for 72 h. The IC50s of paclitaxel was determined with or without 2 μM LY2228820 after 72 h treatment. G. Cell morphology

of Bads-200 was imaged by inverted microscopic examination after different treatments for 72 h. H. Colony formation of Bads-200 with various treatments. Data are shown as mean ± SD. ***P < 0.001. CTL, control; LY, 2 μM LY2228820; PTX, 500 nM paclitaxel; LY + PTX, combination of 2 μM LY2228820 and 500 nM paclitaxel; VB, 500 nM vinorelbine; LY + VB, combination of 2 μM LY2228820 and 500 nM vinorelbine.

Table 1. LY2228820 induces synergistic effects with AMT agents in Bads-200 and Bats-72

Drug	LY2228820 (μM)	Bads-200		Bats-72	
		IC50 (nM)	RI[a]	IC50 (nM)	RI
Paclitaxel	+0	1501 ± 68.5	-	233.7 ± 21.8	-
	+2	420.7 ± 30.7	3.57	46.4 ± 5.6	5.03
Vinorelbine	+0	3388.7 ± 390.5	-	1126.7 ± 207	-
	+2	388 ± 18.5	8.73	260.3 ± 90.2	4.32
Doxorubicin	+0	8710 ± 1656.9	-	3490 ± 276.2	-
	+2	8440 ± 2511.9	1.03	3360 ± 310	1.04
Mitomycin	+0	9289 ± 1437.8	-	7566.7 ± 133.5	-
	+2	8690 ± 3891.3	1.07	7970.3 ± 414.5	0.95

[a]RI (reversal index) was determined by the IC50 in the absence of LY2228820 divided by the IC50 in the presence of LY2228820.

induce a comparable level of G2/M arrest or apoptosis with the co-administration regime. Subsequently, the expression level of several regulatory proteins associated with G2/M arrest and apoptosis were analyzed by western blot. As depicted in **Figure 2C**, **2D**, a notable increase in the expression of Cyclin B1 and a decrease in expression of Cdc2 were observed in the co-administration group compared with paclitaxel or vinorelbine alone. Also, the co-administration led to a stronger cleavage of caspase-3 and poly ADP-ribose polymerase (PARP). In conclusion, LY2228820 enhances G2/M arrest and apoptosis induced by AMT agents.

The co-administration with LY2228820 improves the effectiveness of paclitaxel in Bats-72 xenograft models without additional adverse effects

The previous results indicated that LY22288-20 induces synergistic effect with AMT agents *in vitro*. This raised a clinical concern regarding whether this phenomenon could be replicated *in vivo*. As shown in **Figure 3A-C**, while control and monotherapy groups had no significant difference in tumor volume, the xenografts of co-administration group were significantly smaller than the other three groups (n = 6, P < 0.001). These results confirmed synergistic effect *in vivo*. The mean tumor volumes were 800 ± 109, 751 ± 112, 687 ± 119, 196 ± 49 mm^3, and mean tumor weights were 0.58 ± 0.08, 0.54 ± 0.10, 0.51± 0.12, 0.26 ± 0.03 g. As depicted in **Figure 3C**, when co-treated with LY2228820, the inhibition rate of paclitaxel was significantly elevated from 11.5% to 56.2% (n = 6, P < 0.001). Furthermore, resected tumors were analyzed by immunohistochemistry staining with the antibody against Ki-67. When co-treated with LY2228820 and paclitaxel, the number of intratumoral Ki-67-positive cells significantly decreased compared with the other three groups (**Figure 3E**).

Notably, the co-administration of LY2228820 and paclitaxel did not lead to any significant effects on the body weight of mice (**Figure 3D**). Typically, high doses of paclitaxel have closely been related to hepatotoxicity and nephrotoxicity in preclinical studies and clinical settings [11-13]. Therefore, the liver and kidney tissues of mice were resected and underwent careful histological examination. H&E staining showed that the combination therapy did not lead to significant pathological difference in the hepatic lobule, interlobular vein, glomerulus or uriniferous tubule, indicating no toxic effects on the liver or kidney (**Figure 3F**). Furthermore, the co-treatment of LY2228820 and paclitaxel did not cause significant increase of ALT, AST and creatinine levels (**Figure 3G**). Collectively, these results demonstrated that co-administration with LY2228820 improves the effectiveness of paclitaxel at relatively low dosage in Bats-72 xenograft models without severe adverse effects frequently induced by high dose paclitaxel.

LY2228820 sensitizes cancer cells to AMT agents independent of P-gp

In our previous study, an up-regulation of P-gp protein was observed in Bads-200 cell [9]. We then aimed to investigate whether such synergistic effect was caused by the down-regulation

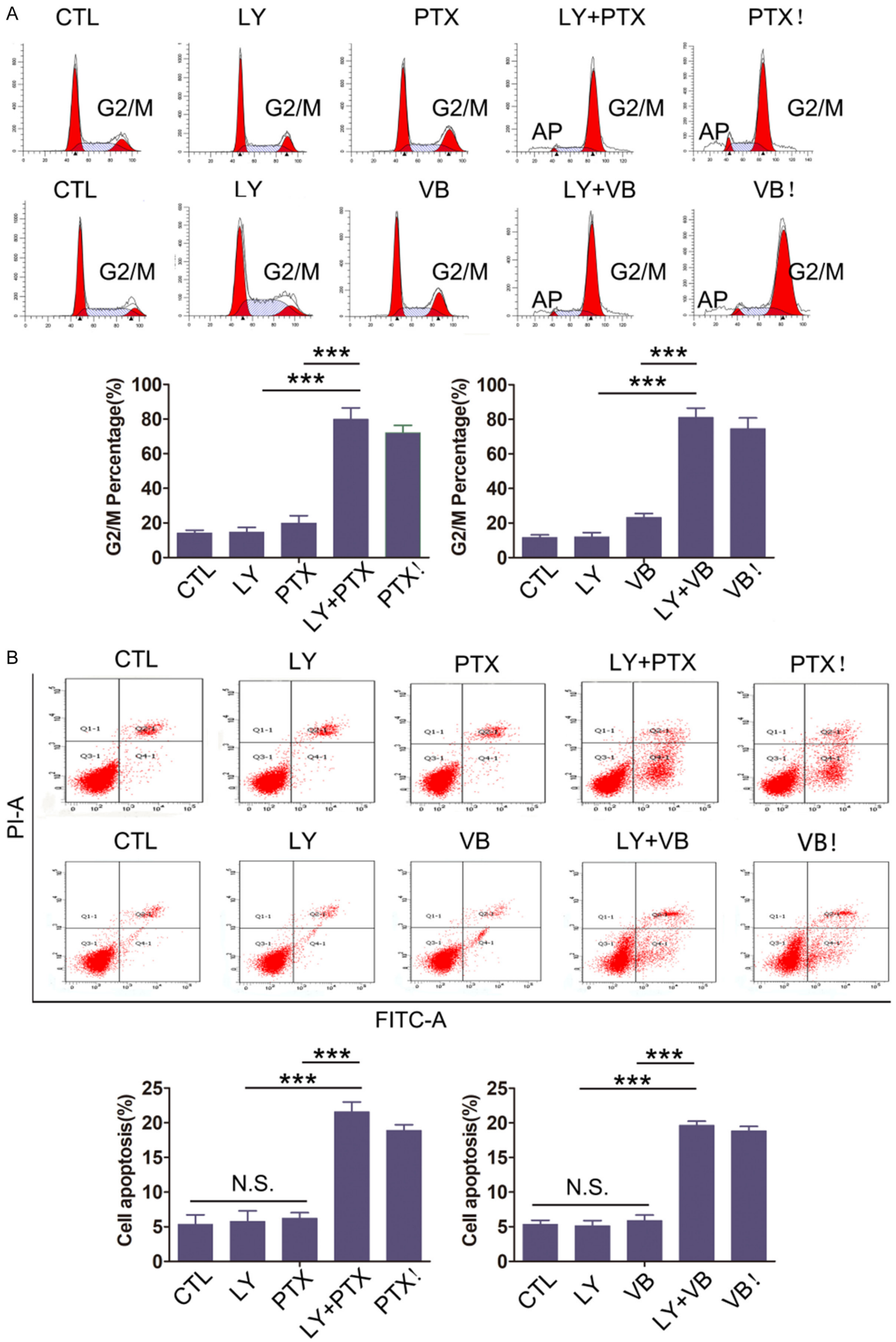
A
CTL
LY
PTX
LY+PTX
PTX!
G2/M
AP
CTL
LY
VB
LY+VB
VB!
G2/M
AP
***
***
G2/M Percentage(%)
100
80
60
40
20
0
CTL
LY
PTX
LY+PTX
PTX!
VB
LY+VB
VB!
B
CTL
LY
PTX
LY+PTX
PTX!
CTL
LY
VB
LY+VB
VB!
PI-A
FITC-A
Q1-1
Q2-1
Q3-1
Q4-1
***
***
Cell apoptosis(%)
25
20
15
10
5
0
N.S.
CTL
LY
PTX
LY+PTX
PTX!
VB
LY+VB
VB!

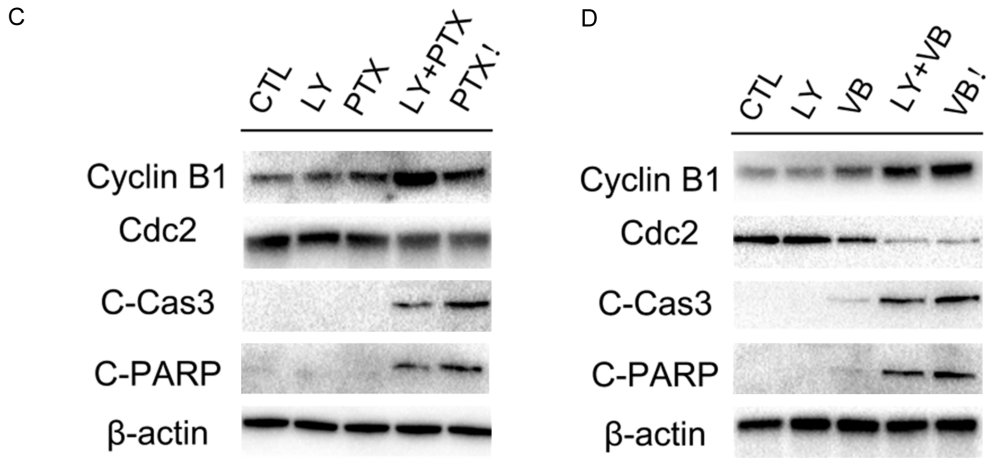

Figure 2. LY2228820 enhances G2/M arrest and apoptosis induced by AMT agents. A. Cell cycle analysis of Bads-200 after different treatments for 72 h. B. The proportion of apoptotic cells of Bads-200 with various administrations for 72 h was tested. C, D. Western blot analysis of Cyclin B1, Cdc2, C-Cas3, and C-PARP proteins in Bads-200 after different treatments for 72 h. AP peaks represent the population of apoptotic cells. Data are shown as mean ± SD. N.S., $P > 0.05$; ***$P < 0.001$. CTL, control; LY, 2 μM LY2228820; PTX, 500 nM paclitaxel; LY + PTX, combination of 2 μM LY2228820 and 500 nM paclitaxel; PTX!, 2000 nM paclitaxel; VB, 500 nM vinorelbine; LY + VB, combination of 2 μM LY2228820 and 500 nM vinorelbine; VB!, 5000 nM vinorelbine.

of P-gp protein or the inhibition of its function. Western blot showed that LY2228820 did not influence the expression of P-gp protein (**Figure 4A**). Next, we performed Rh123 intracellular accumulation and efflux assay. As shown in **Figure 4B** and **4C**, compared with ROD group, the amount of intracellular Rh123 exhibited no difference after the co-treatment with LY2228820 but was significantly elevated when co-treated with verapamil (VRP), a positive control [14]. Furthermore, Pgp-Glo™ Assay confirmed that LY2228820 did not affect the ATPase activity of P-gp (**Figure 4D**), indicating that LY2228820 is not a substrate of P-gp. Doxorubicin and mitomycin have a high affinity for P-gp, and **Figure 4E** showed that LY2228820 has an insignificant impact on the sensitivity of Bads200 to these two drugs. Moreover, the co-administration with LY2228820 significantly sensitized Bcap37and HCC-LM3, two cell lines with no expression of P-gp, to paclitaxel (**Figure 4F**). These findings suggested that LY2228820 could sensitize cancer cells to AMT agents independent of P-gp.

The co-administration with LY2228820 promotes paclitaxel-induced mitochondrial cell death by altering the P38/HSP-27 signaling axis

As LY2228820 is a potent and selective kinase inhibitor of P38 MAPK, we tested several signaling proteins associated with P38 MAPK pathway to analyze their involvement in the synergistic effect. As previously shown, the co-administration of LY2228820 (2 μM) with paclitaxel (500 nM) could induce a comparable level of apoptosis with monotherapy of 2000 nM paclitaxel *in vitro*. However, the P38/HSP27 signaling axis was differently regulated in cells undergoing the combination treatment, compared to cells treated with 2000 nM paclitaxel alone (**Figure 5A**). The expression level of p-MK-K3, p-P38 and p-MK2 were only remarkably increased in LY + PTX group, while the protein level of p-HSP27 (Ser78) was notably elevated only in PTX! (2000 nM PTX) group. Interestingly, the phosphorylation of HSP27 at Ser78 was completely inhibited in LY + PTX group compared to PTX! group. The results obtained with vinorelbine treatment were consistent with those treated with paclitaxel (**Figure 5B**). It has been reported that the phosphorylation of HSP27 protects cells from oxidative stress and thus its suppression is involved in mitochondria-related apoptosis [15-17]. We measured the mitochondrial membrane potential (MMP) using JC-1 assay to analyze whether LY2228820 promoted paclitaxel-induced mitochondrial cell death via inhibition of p-HSP27. As depicted in **Figure 5C**, **5D**, there were no significant differences in MMP between LY and PTX groups compared to the control group.

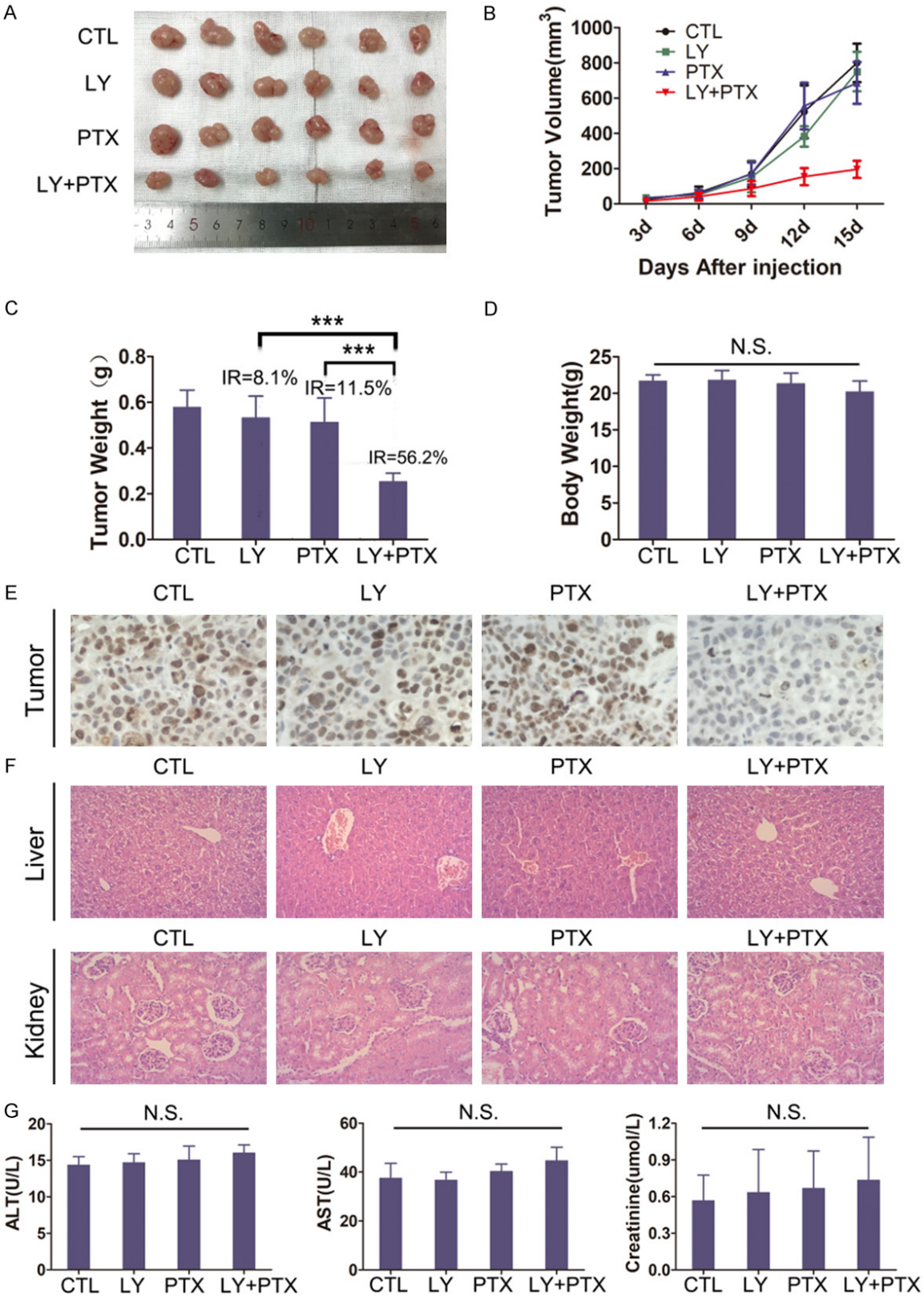

Figure 3. The co-administration with LY2228820 improves the effectiveness of paclitaxel in MDR tumor xenograft without additional adverse effects. Nude mice bearing Bats-72 tumors were treated with paclitaxel +/- LY2228820. A. Tumor mass of four groups with different treatments. B. Tumor volume of four groups in the treatment process. C, D. Tumor weight and body weight of mice at the end of experiments. E, F. immunohistochemical staining (× 200)

of tumors and histological analysis (× 200) of liver and kidney were performed. G. Serum ALT, AST and creatinine levels were measured in each group. Data are shown as mean ± SD. N.S., P > 0.05; ***P < 0.001. CTL, control; LY, LY2228820; PTX, paclitaxel; LY + PTX, co-administration of LY2228820 and paclitaxel; IR, inhibition rate.

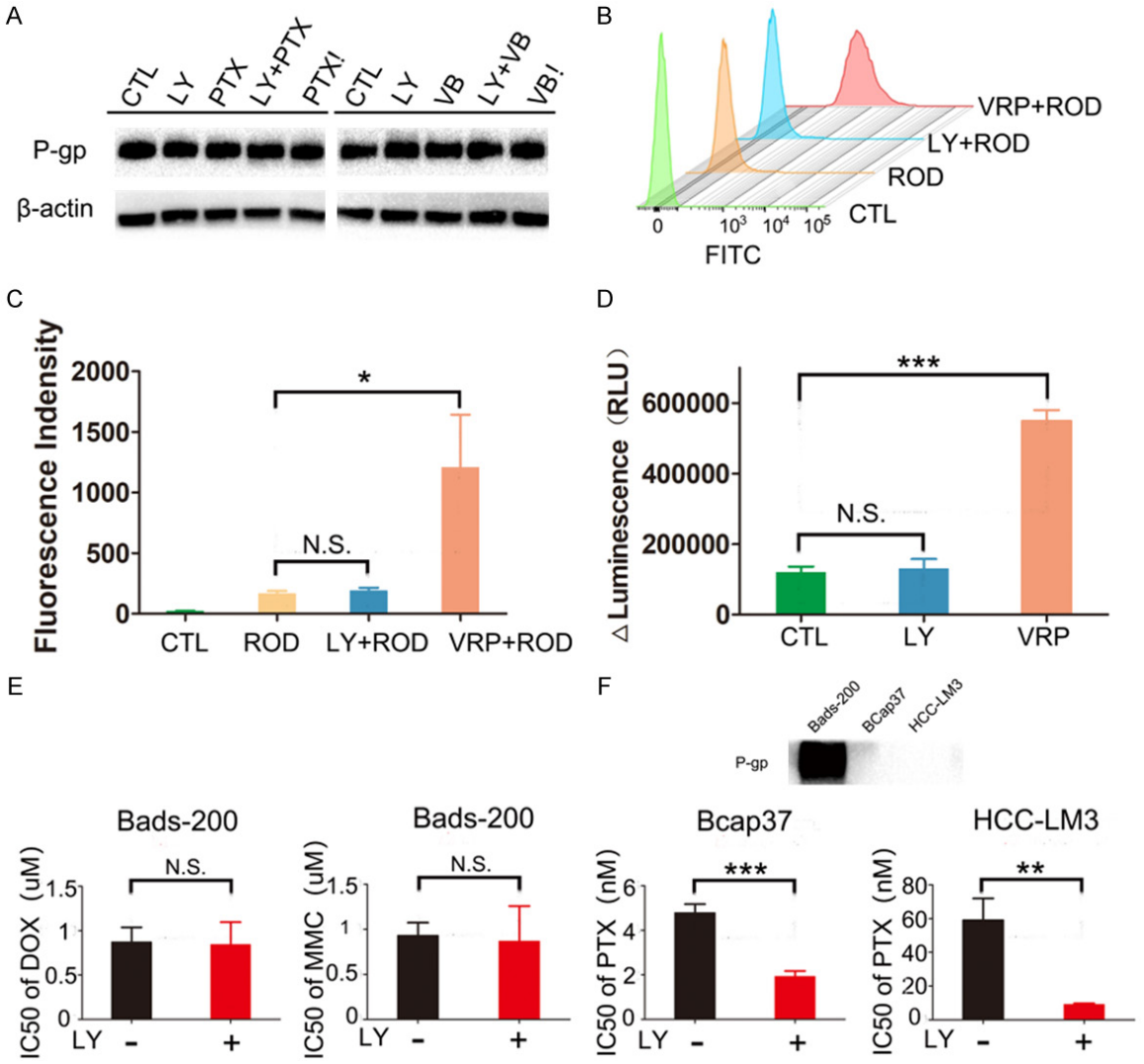

Figure 4. LY2228820 sensitizes cancer cells to AMT agents independent of P-gp. A. Western blot analysis of P-gp proteins in Bads-200 after different treatments for 72 h. CTL, control; LY, 2 μM LY2228820; PTX, 500 nM paclitaxel; LY + PTX, combination of 2 μM LY2228820 and 500 nM paclitaxel; PTX!, 2000 nM paclitaxel; VB, 500 nM vinorelbine; LY + VB, combination of 2 μM LY2228820 and 500 nM vinorelbine; VB!, 5000 nM vinorelbine. B, C. Intracellular Rh123 fluorescence intensity in Bads-200 with different treatments was determined. CTL, control; Rod, treatment with 5 μM rhodamine 123 for 0.5 h; LY + ROD, pre-incubation with 2 μM LY2228820 for 3 h, then treated with 5 μM rhodamine 123 for 0.5 h; VRP, pre-incubation with 20 μM verapamil for 3 h, then treated with 5 μM rhodamine 123 for 0.5 h. D. The effect of LY2228820 on the ATPase activity of P-glycoprotein was measured. LY, 2 μM LY2228820; VRP, 20 μM verapamil. E. The IC50s of doxorubicin and mitomycin with or without 2 μM LY2228820 after 72 h treatment of Bads-200 were determined. F. The expression of P-gp in Bads-200, BCap37 and HCC-LM3 cells were detected by western blot. The IC50s of paclitaxel with or without 2 μM LY2228820 after 72 h treatment of Bcap37 and HCC-LM3 were determined. Data are shown as mean ± SD. N.S., P > 0.05; *P < 0.05; **P < 0.01; ***P < 0.001.

Compared with the PTX group, MMP was significantly reduced in both LY + PTX and PTX! groups (P < 0.001), indicating higher levels of mitochondria-related apoptosis. Moreover, more Cytochrome C was released into the cytoplasm from mitochondria in LY + PTX and PTX! groups (**Figure 5E**). In summary, the co-administration with LY2228820 could promote mitochondrial cell death by altering P38/HSP-27 signaling axis.

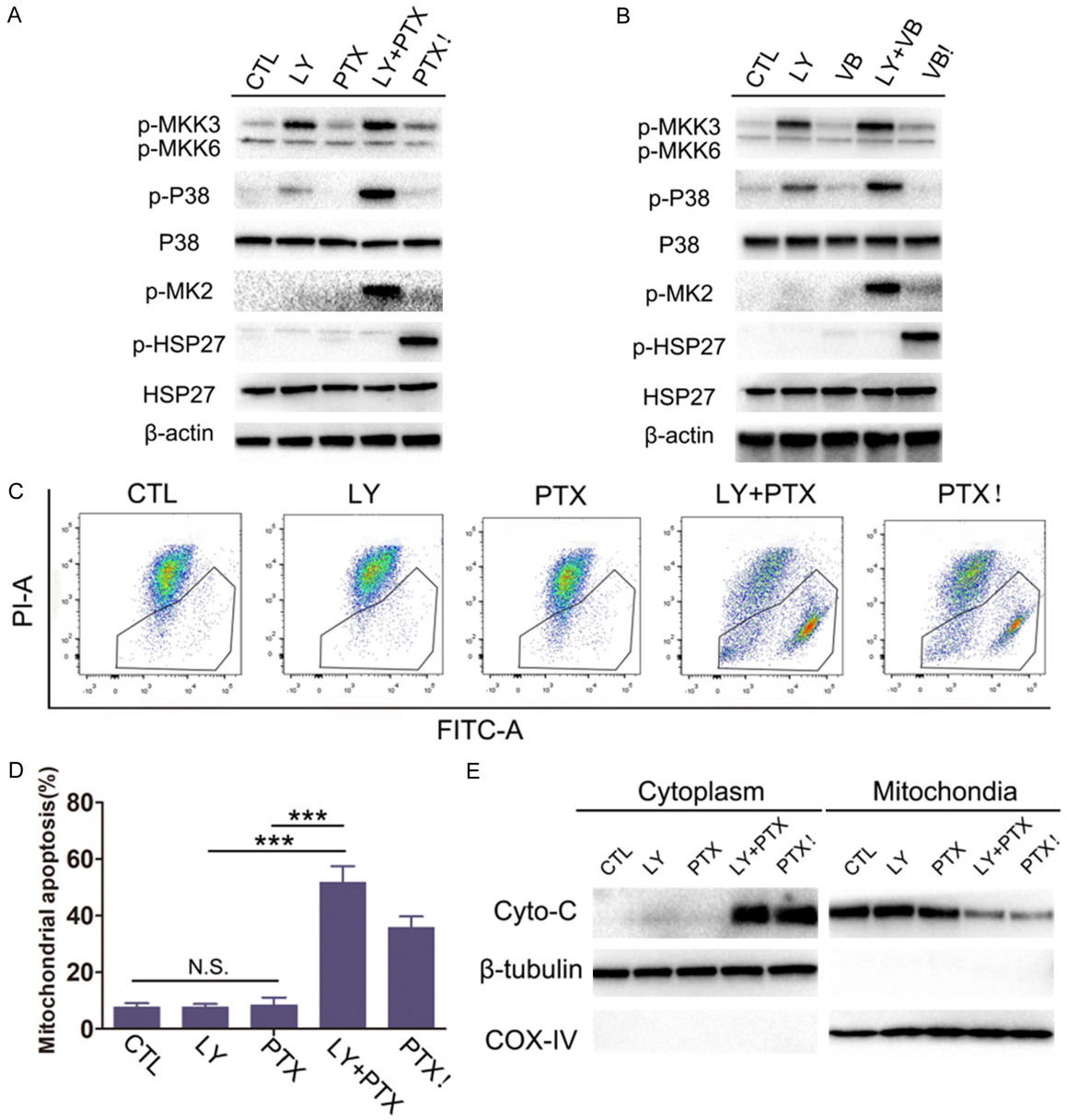

Figure 5. The co-administration with LY2228820 promotes paclitaxel-induced mitochondrial cell death by altering P38 MAPK pathway. A, B. Western blot analysis of p-MKK3/6, p-P38, P38, p-MK2, HSP27 and p-HSP27 proteins in Bads-200 after different treatments for 72 h. C, D. MMP was analyzed by FCM by JC-1 assays in Bads-200 after different treatments for 72 h. E. The subcellular localization of Cytochrome C was assessed by western blot after cytoplasm and mitochondrial fraction of Bads-200 with various different treatments for 72 h. MMP, mitochondrial membrane potential; Data are shown as mean ± SD. N.S., $P > 0.05$; ***$P < 0.001$. CTL, control; LY, 2 μM LY2228820; PTX, 500 nM paclitaxel; LY + PTX, combination of 2 μM LY2228820 and 500 nM paclitaxel; PTX!, 2000 nM paclitaxel; VB, 500 nM vinorelbine; LY + VB, combination of 2 μM LY2228820 and 500 nM vinorelbine; VB!, 5000 nM vinorelbine.

LY2228820 causes synergistic effect with AMT drugs by down-regulating the phosphorylation of HSP27

We aimed to further explore the role of p-HSP-27 in AMT drugs mediated mitochondrial cell death in tumor cells. As the concentration of paclitaxel or vinorelbine increased, the expression of p-HSP27 elevated consistently with the apoptotic marker C-PARP (**Figure 6A**, **6B**). This suggested that p-HSP27 might promote AMT drug-induced cell apoptosis or exert a protec-

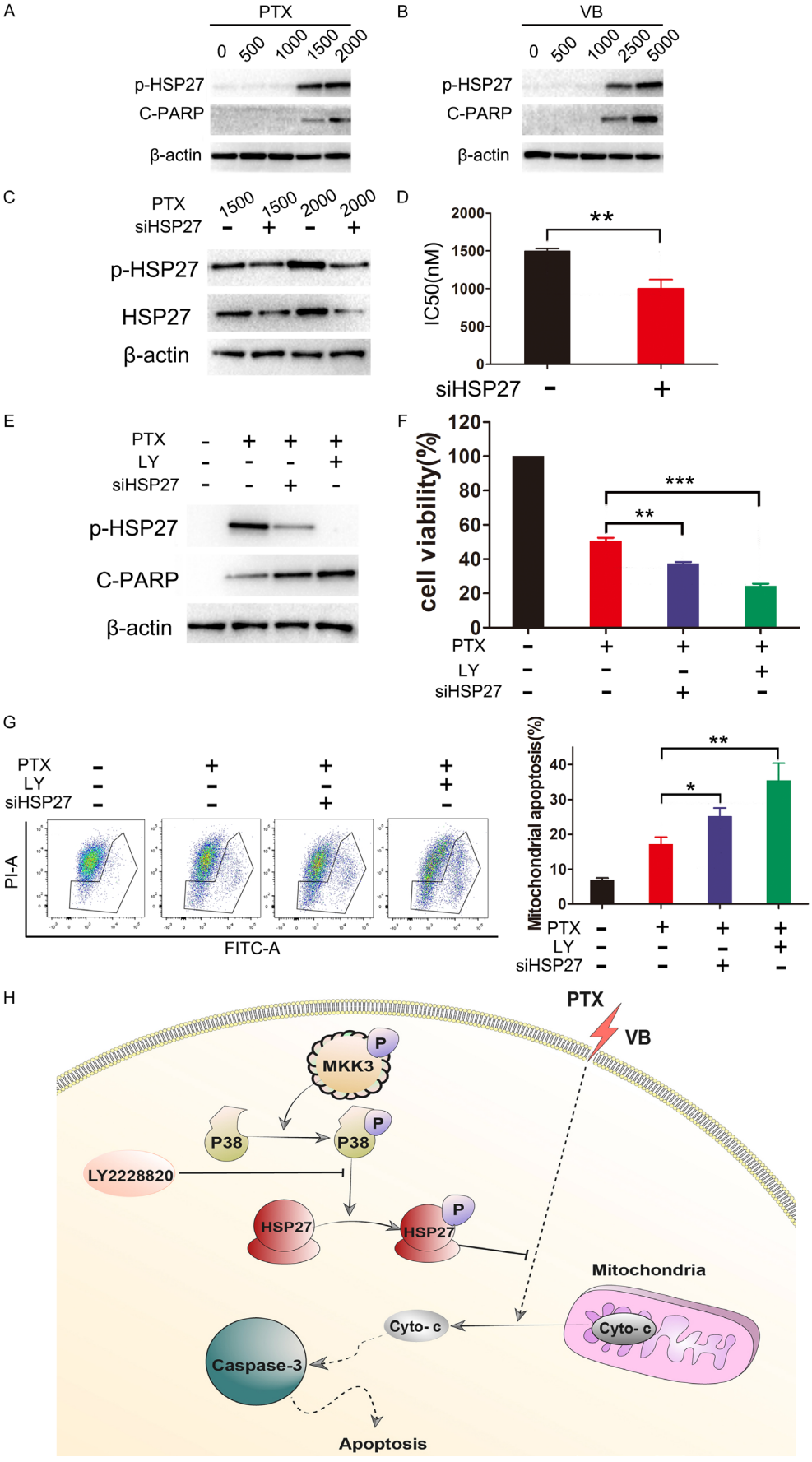
A
PTX
0 500 1000 1500 2000
p-HSP27
C-PARP
β-actin
B
VB
0 500 1000 2500 5000
p-HSP27
C-PARP
β-actin
C
PTX 1500 1500 2000 2000
siHSP27 - + - +
p-HSP27
HSP27
β-actin
D
IC50(nM)
2000
1500
1000
500
0
**
siHSP27 - +
E
PTX - + + +
LY - - - +
siHSP27 - - + -
p-HSP27
C-PARP
β-actin
F
cell viability(%)
120
100
80
60
40
20
0
***
**
PTX - + + +
LY - - - +
siHSP27 - - + -
G
PTX - + + +
LY - - - +
siHSP27 - - + -
PI-A
FITC-A
Mitochondrial apoptosis(%)
40
30
20
10
0
**
*
PTX - + + +
LY - - - +
siHSP27 - - + -
H
PTX
VB
MKK3
P
P38
P
LY2228820
HSP27
P
Mitochondria
Cyto- c
Cyto- c
Caspase-3
Apoptosis

Figure 6. LY2228820 causes synergistic effect with AMT drugs by down-regulating the phosphorylation of HSP27. A, B. Bads-200 was treated with ascending concentrations of paclitaxel (0-2000 nM) and vinorelbine (0-5000 nM) for 72 h, and then the expression of p-HSP27 and C-PARP was analyzed by western blot. C. Bads-200 was treated with relatively high concentration of paclitaxel (1500 and 2000 nM) for 72 h in the presence or absence of HSP27 siRNA, and then the expression of p-HSP27 and HSP27 was analyzed by western blot. D. The IC50s of paclitaxel in Bads-200 were determined after 72 h treatment in the presence or absence of HSP27 siRNA. E-G. Bads-200 cells were divided into four groups with different treatment for 72 h: control, 1500 nM PTX, 1500 nM PTX + HSP27 siRNA and 1500 nM PTX + 2 μM LY2228820. The expression of p-HSP27 and C-PARP was analyzed by western blot. Cell viability of each group was assessed by MTT assay. MMP was analyzed by JC-1 assays. Data are shown as mean ± SD. *P < 0.05; **P < 0.01; ***P < 0.001; H. Through inhibiting the phosphorylation of HSP27, LY2228820 causes synergistic effect with AMT drugs via promoting mitochondrial cell death. PTX, paclitaxel; VB, vinorelbine.

tive response against AMT drug-mediated cell death. To ascertain whether p-HSP27 is a pro-apoptosis or anti-apoptosis factor in the AMT pharmacotherapy, we compared the IC50 values of paclitaxel in the presence or absence of siHSP27. The results indicated that the down-regulation of p-HSP27 via HSP27 knockdown could sensitize Bads-200 cells to paclitaxel. The IC50 values of paclitaxel decreased from 1500 nM to 996.3 nM when cells were transfected with HSP27 siRNA (**Figure 6C**, **6D**). These results demonstrated that p-HSP27 could mediate a protective response against AMT drugs in tumor cells. Next, Bads-200 cells were treated with four regimes: control, 1500 nM PTX, 1500 nM PTX + HSP27 siRNA and 1500 nM PTX + 2 μM LY2228820. The cleavage level of PARP, p-HSP27, cell viability, and mitochondrial potential were evaluated in each group. The expression of p-HSP27 progressively decreased in 1500 nM PTX, 1500 nM PTX + HSP27 siRNA and 1500 nM PTX + 2 μM LY2228820 groups. On the contrary, C-PARP expression progressively increased in these three groups (**Figure 6E**). Compared with the control group, the cell viability in the other three groups decreased to 50.4%, 37.2%, and 24.1%, while the proportion of mitochondrial cell death were 17.06%, 25.17% and 35.37%, respectively (**Figure 6F**, **6G**). These confirmed that the level of p-HSP27 was negatively correlated with the severity of cytotoxicity as well as the level of mitochondrial cell death, indicating that p-HSP27 indeed exerts anti-apoptotic effect with PTX treatment. Taken together, LY2228820 induces synergistic effect with paclitaxel by blocking the p-HSP27-mediated protective response against AMT drugs in tumor cells (**Figure 6H**).

Discussion

Although chemotherapy is currently one of the most frequently used treatment for cancer patients, it is often associated with the risks of chemo-resistance as well as other side effects including cardiotoxicity, nephrotoxicity, hepatotoxicity and gastrointestinal toxicity [18]. To overcome such obstacles, novel combined chemotherapeutic treatments are in urgent need to achieve continuous improvements in long-term survival and quality of life [19]. Compared with normal cells, cancers cells have distinct epigenetic, genetic alterations and microenvironment, leading to the need for specific molecular targets. In this study, we identified that P38/MAPK inhibitor LY2228820 could achieve synergistic anti-cancer effects with low doses of paclitaxel and vinorelbine by enhancing G2/M arrest and mitochondrial apoptosis in a p38/MAPK-HSP-27 signaling axis-dependent manner. Xenograft assays showed that this combination therapy could suppress the growth of paclitaxel-resistant cells with a tolerable dosage of paclitaxel *in vivo* to avoid severe systematic toxicity. This combination therapy might be effective for cancer patients unresponsive to maximal dosage of AMT chemotherapy or those who cannot tolerate the systematic toxicity of these agents in clinic.

P-glycoprotein (P-gp) is the major ATP-dependent efflux pump responsible for resistance to chemotherapy agents including AMT [20]. In order to reverse P-gp-mediated chemotherapy resistance, many agents have been investigated in clinical trials, including verapamil, quinidine, cyclosporine A, PSC-833 [14, 21-23]. However, these inhibitors have not been proven to be effective as chemotherapy sensitizing agents in clinical trials due to the lack of additional survival benefit, as well as their toxicity caused by pharmacological interactions with anticancer drugs and their interference with normal physiological functions including liver and kidney [24]. In contrast, here we showed that LY2228820 could resensitize a P-gp-high-expressing cell line to AMT agents without alter-

ing its P-gp activity. At the same time, our *in vivo* study showed that neither did this combination therapy induce extra toxicity to cause weight loss in animal models, nor did it interfere with liver and kidney functions. Therefore, our finding might offer a safer alternative for patients with high P-gp-expression in the clinical setting.

Moreover, cancers are highly heterogeneous, and the up-regulation of P-gp is not the only mechanism of paclitaxel resistance. For example, both up-regulation and mutation of beta-tubulin have been identified in non-small-cell lung cancer and ovarian cancer patients showing resistance to paclitaxel, among whom P-gp inhibitors might show less potency [25-28]. Other than inducing cell cycle arrest, AMT agents also create mitochondrial stress to kill cancer cells [29, 30]. Mitochondria, the energy factory of eukaryotic cells, might be the key to overcoming drug resistance in certain cancer patients. Triona Ni Chonghaile *et al.* reported that malignant cells showing disrupted mitochondrial homeostasis would respond better to cytotoxic agents, compared to those with undamaged mitochondrial homeostasis in patients with multiple myeloma, acute myelogenous, lymphoblastic leukemia, and ovarian cancer [31]. Thus, it is worth re-evaluating the importance of mitochondrial homeostasis in cancer, which might be the Achilles' heel of cancer cells with variant genetic background relating to drug resistance. Here in this study, LY2228820 sensitizes cancer cells to paclitaxel or vinorelbine by suppressing the phosphorylation of HSP27, a protein involved in mitochondrial homeostasis. Thus, even low doses of paclitaxel combined with LY2228820 could induce significant apoptosis in cancer cells by interfering with mitochondrial homeostasis. The synergistic anti-cancer effects of LY2228820 and AMT agents are still under evaluation in other cells without P-gp overexpression. Our preliminary data suggest that such effect could also exist in P-gp-null breast and liver cancer cell lines (**Figure 4F**), which indicates that LY2228820 might be able to sensitize a wider range of cancer types to AMT agents by priming mitochondria into vulnerable states.

HSP27 is a molecular chaperone highly expressed in many kinds of aggressive cancers, including ovarian cancer, colorectal cancer, and breast cancer [32-34]. It consecutively counteracts the formation of misfolded proteins and allows for correct protein folding when cancer cells are exposed to various stresses, such as chemotherapies and radio therapies. Therefore, high HSP27 expression is associated with resistance to chemotherapies. For example, analysis on biopsies from breast cancer patients treated with chemotherapy showed that nuclear accumulation and high cytoplasmic HSP27 were correlated with shorter disease-free survival time [35]. Moreover, siRNA-mediated down-regulation of HSP27 expression enhanced paclitaxel-induced apoptosis in bladder cancer cells, which is consistent with our observations in this report [36]. Detailed biochemistry analysis showed that HSP27 could be phosphorylated in response to multiple upstream signals through p38 MAPK-MK2 signaling pathway [37]. Unphosphorylated HSP27 aggregated into large oligomer (up to 800 Kda) while phosphorylated HSP27 forms smaller oligomer [38]. Only large oligomers show chaperone activity, while dimerized HSP27 could interact with cytochrome c and prevent the formation of the apoptosome [16, 39]. Here we showed that LY2228820 suppressed phosphorylation of HSP27 and induced stronger paclitaxel-induced apoptosis, which might be attributed to blockage of the protein-protein interaction between cytochrome c and phosphorylated HSP27.

Aside from sensitizing paclitaxel-resistant breast cancer cells to AMT therapies, LY2228820 can also enhance bortezomib-induced cytotoxicity and inhibit osteoclastogenesis in multiple myeloma [40, 41]. Moreover, it suppresses angiogenesis which is critical for the growth as well as metastasis of solid tumors [42]. Considering the central role of the p38/MAPK pathway in stress response against various forms of cancer therapies, as well as the production of several cytokines inducing angiogenesis and immune tolerance, it is worth comprehensively analyzing the effect of combining LY2228820 with a broader category of clinically available therapeutics. Here we noticed that doxorubicin and mitomycin could not function synergistically with LY2228820. Such selectivity still requires further investigation. Nonetheless, the change in angiogenesis should also be evaluated in combination therapy *in vivo*.

In summary, synergistic anti-cancer chemotherapy offers a novel strategy for improving the therapeutic efficacy of chemotherapy drugs by achieving a better balance between efficacy and toxicity. Without further systematic toxicity, a non-toxic dosage of LY2228820 co-administrated with a low-toxic dosage of AMT agents could produce synergistic anti-cancer effects via promotion of mitochondrial death. This new combination regime could be advantageous in patients who show little response to the maximal dosage of AMT chemotherapy, as well as those unable to tolerate the systematic toxicity of these agents in clinic.

Acknowledgements

This research was supported by Zhejiang Provincial Natural Science Foundation (LY18H16-0017); Fundamental Research Funds for the Central Universities (2019XZZX005-1-08); Innovative Research Groups of National Natural Science Foundation of China (No. 81721091); National S&T Major Project (No. 2017ZX102-03205); Zhejiang International Science and Technology Cooperation Project (N0.2016C0-4003); Zhejiang Provincial Natural Science Foundation (LY15H080002).

Disclosure of conflict of interest

None.

Address correspondence to: Shusen Zheng and Donghai Jiang, Department of Surgery, Division of Hepatobiliary and Pancreatic Surgery, First Affiliated Hospital, School of Medicine, Zhejiang University, Hangzhou 310000, Zhejiang Province, China. E-mail: shusenzheng@zju.edu.cn (SSZ); jdh8499@zju.edu.cn (DHJ)

References

[1] Chabner BA and Roberts TG Jr. Chemotherapy and the war on cancer. Nat Rev Cancer 2005; 5: 65-72.

[2] Kazandjian D, Blumenthal GM, Yuan W, He K, Keegan P and Pazdur R. FDA approval of gefitinib for the treatment of patients with metastatic egfr mutation-positive non-small cell lung cancer. Clin Cancer Res 2016; 22: 1307-12.

[3] Nurgalieva Z, Liu CC and Du XL. Chemotherapy use and risk of bone marrow suppression in a large population-based cohort of older women with breast and ovarian cancer. Med Oncol 2011; 28: 716-725.

[4] Mitchell EP. Gastrointestinal toxicity of chemotherapeutic agents. Semin Oncol 2006; 33: 106-120.

[5] Mansoori B, Mohammadi A, Davudian S, Shirjang S and Baradaran B. The different mechanisms of cancer drug resistance: a brief review. Adv Pharm Bull 2017; 7: 339-348.

[6] Minor DR, Puzanov I, Callahan MK, Hug BA and Hoos A. Severe gastrointestinal toxicity with administration of trametinib in combination with dabrafenib and ipilimumab. Pigment Cell Melanoma Res 2015; 28: 611-2.

[7] Johannessen TC, Hasan-Olive MM, Zhu H, Denisova O, Grudic A, Latif MA, Saed H, Varughese JK, Røsland GV, Yang N, Sundstrøm T, Nordal A, Tronstad KJ, Wang J, Lund-Johansen M, Simonsen A, Janji B, Westermarck J, Bjerkvig R and Prestegarden L. Thioridazine inhibits autophagy and sensitizes glioblastoma cells to temozolomide. Int J Cancer 2019; 144: 1735-1745.

[8] Frederiks CN, Lam SW, Guchelaar HJ and Boven E. Genetic polymorphisms and paclitaxel- or docetaxel-induced toxicities: a systematic review. Cancer Treat Rev 2015; 41: 935-50.

[9] Jiang D, Sui M, Zhong W, Huang Y and Fan W. Different administration strategies with paclitaxel induce distinct phenotypes of multidrug resistance in breast cancer cells. Cancer Lett 2013; 335: 404-411.

[10] Bauer JA, Duan Z, Choy E and Hornicek FJ. NSC23925, identified in a high-throughput cell-based screen, reverses multidrug resistance. PLoS One 2009; 4: e7415.

[11] Grigorian A and O'Brien CB. Hepatotoxicity secondary to chemotherapy. J Clin Transl Hepatol 2014; 2: 95-102.

[12] du Bois A, Schlaich M, Lück HJ, Mollenkopf A, Wechsel U, Rauchholz M and Bauknecht T, Meerpohl HG. Evaluation of neurotoxicity induced by paclitaxel second-line chemotherapy. Support Care Cancer 1999; 7: 354-61.

[13] Kim SC, Shim YH, Bang JOH, Kim SW, Seo MH and Kim DW. In vivo evaluation of polymeric micellar paclitaxel formulation: toxicity and efficacy. J Control Release 2001; 72: 191-202.

[14] Pauli-Magnus C, von Richter O, Burk O, Ziegler A, Mettang T, Eichelbaum M and Fromm MF. Characterization of the major metabolites of verapamil as substrates and inhibitors of P-glycoprotein. J Pharmacol Exp Ther 2000; 293: 376-82.

[15] Arrigo AP. Hsp27: novel regulator of intracellular redox state. IUBMB Life 2001; 52: 303-7.

[16] Benn SC, Perrelet D, Kato AC, Scholz J, Decosterd I, Mannion RJ, Bakowska JC and Woolf

CJ. Hsp27 upregulation and phosphorylation is required for injured sensory and motor neuron survival. Neuron 2002; 36: 45-56.
[17] Carmen G, Mathilde B, Celine D, Yael Z, Elise S and Guido K. Heat shock proteins 27 and 70: anti-apoptotic proteins with tumorigenic properties. Cell Cycle 2006; 5: 2592-2601.
[18] Xiao Q, Zhu W, Feng W, Lee SS, Leung AW, Shen J, Gao L and Xu C. A review of resveratrol as a potent chemoprotective and synergistic agent in cancer chemotherapy. Front Pharmacol 2018; 9: 1534.
[19] Domvri K, Zarogoulidis K, Zogas N, Zarogoulidis P, Petanidis S, Porpodis K, Kioseoglou E and Hohenforst-Schmidt W. Potential synergistic effect of phosphodiesterase inhibitors with chemotherapy in lung cancer. J Cancer 2017; 8: 3648-3656.
[20] Ling V and Thompson LH. Reduced permeability in CHO cells as a mechanism of resistance to colchicine. J Cell Physiol 1974; 83: 103-16.
[21] Jain R, Majumdar S, Nashed Y, Pal D and Mitra AK. Circumventing P-glycoprotein-mediated cellular efflux of quinidine by prodrug derivatization. Mol Pharm 2004; 1: 290-9.
[22] List AF, Kopecky KJ, Willman CL, Head DR, Slovak ML, Douer D, Dakhil SR and Appelbaum FR. Cyclosporine inhibition of P-glycoprotein in chronic myeloid leukemia blast phase. Blood 2002; 100: 1910-1912.
[23] Tidefelt U, Liliemark J, Gruber A, Liliemark E, Sundman-Engberg B, Juliusson G, Stenke L, Elmhorn-Rosenborg A, Möllgård L, Lehman S, Xu D, Covelli A, Gustavsson B and Paul C. P-glycoprotein inhibitor valspodar (PSC 833) increases the intracellular concentrations of daunorubicin in vivo in patients with P-glycoprotein-positive acute myeloid leukemia. J Clin Oncol 2000; 18: 1837-44.
[24] Abdallah HM, Al-Abd AM, El-Dine RS and El-Halawany AM. P-glycoprotein inhibitors of natural origin as potential tumor chemo-sensitizers: a review. J Adv Res 2015; 6: 45-62.
[25] Atjanasuppat K, Lirdprapamongkol K, Jantaree P and Svasti J. Non-adherent culture induces paclitaxel resistance in H460 lung cancer cells via ERK-mediated up-regulation of βIVa-tubulin. Biochem Biophys Res Commun 2015; 466: 493-8.
[26] Duran GE, Wang YC, Moisan F, Francisco EB and Sikic BI. Decreased levels of baseline and drug-induced tubulin polymerisation are hallmarks of resistance to taxanes in ovarian cancer cells and are associated with epithelial-to-mesenchymal transition. Br J Cancer 2017; 116: 1318-1328.
[27] Monzó M, Rosell R, Sánchez JJ, Lee JS, O'Brate A, González-Larriba JL, Alberola V, Lorenzo JC, Núñez L, Ro JY and Martín C. Paclitaxel resistance in non–small-cell lung cancer associated with beta-tubulin gene mutations. J Clin Oncol 1999; 17: 1786-93.
[28] Giannakakou P, Sackett DL, Kang YK, Zhan Z, Buters JT, Fojo T and Poruchynsky MS. Paclitaxel-resistant human ovarian cancer cells have mutant β-tubulins that exhibit impaired paclitaxel-driven polymerization. J Biol Chem 1997; 272: 17118-25.
[29] Pieniążek A, Czepas J, Piasecka-Zelga J, Gwoździński K and Koceva-Chyła A. Oxidative stress induced in rat liver by anticancer drugs doxorubicin, paclitaxel and docetaxel. Adv Med Sci 2013; 58: 104-11.
[30] Sugimura M, Sagae S, Ishioka Si, Nishioka Y, Tsukada K and Kudo R. Mechanisms of paclitaxel-induced apoptosis in an ovarian cancer cell line and its paclitaxel-resistant clone. Oncology 2004; 66: 53-61.
[31] Ni Chonghaile T, Sarosiek KA, Vo TT, Ryan JA, Tammareddi A, Moore Vdel G, Deng J, Anderson KC, Richardson P, Tai YT, Mitsiades CS, Matulonis UA, Drapkin R, Stone R, Deangelo DJ, McConkey DJ, Sallan SE, Silverman L, Hirsch MS, Carrasco DR and Letai A. Pretreatment mitochondrial priming correlates with clinical response to cytotoxic chemotherapy. Science 2011; 334: 1129-1133.
[32] Bauer K, Nitsche U, Slotta-Huspenina J, Drecoll E, von Weyhern CH, Rosenberg R, Höfler H and Langer R. High HSP27 and HSP70 expression levels are independent adverse prognostic factors in primary resected colon cancer. Cell Oncol 2012; 35: 197-205.
[33] Kang SH, Kang KW, Kim KH, Kwon B, Kim SK, Lee HY, Kong SY, Lee ES, Jang SG and Yoo BC. Upregulated HSP27 in human breast cancer cells reduces Herceptin susceptibility by increasing Her2 protein stability. BMC Cancer 2008; 8: 286.
[34] Langdon SP, Rabiasz GJ, Hirst GL, King RJ, Hawkins RA, Smyth JF and Miller WR. Expression of the heat shock protein HSP27 in human ovarian cancer. Clin Cancer Res 1995; 1: 1603-9.
[35] Vargas-Roig LM, Gago FE, Tello O, Aznar JC and Ciocca DR. Heat shock protein expression and drug resistance in breast cancer patients treated with induction chemotherapy. Int J Cancer 1998; 79: 468-75.
[36] Kamada M, So A, Muramaki M, Rocchi P, Beraldi E and Gleave M. Hsp27 knockdown using nucleotide-based therapies inhibit tumor growth and enhance chemotherapy in human bladder cancer cells. Mol Cancer Ther 2007; 6: 299-308.
[37] Zheng C, Lin Z, Zhao ZJ, Yang Y, Niu H and Shen X. MAPK-activated protein kinase-2 (MK2)-mediated formation and phosphorylа-

tion-regulated dissociation of the signal complex consisting of p38, MK2, Akt, and Hsp27. J Biol Chem 2006; 281: 37215-26.

[38] Rogalla T, Ehrnsperger M, Preville X, Kotlyarov A, Lutsch G, Ducasse C, Paul C, Wieske M, Arrigo AP, Buchner J, Gaestel M. Regulation of Hsp27 oligomerization, chaperone function, and protective activity against oxidative stress/tumor necrosis factor α by phosphorylation. J Biol Chem 1999; 274: 18947-56.

[39] Bruey JM, Ducasse C, Bonniaud P, Ravagnan L, Susin SA, Diaz-Latoud C, Gurbuxani S, Arrigo AP, Kroemer G, Solary E and Garrido C. Hsp27 negatively regulates cell death by interacting with cytochrome c. Nature Cell Biology 2000; 2: 645-652.

[40] Hideshima T, Podar K, Chauhan D, Ishitsuka K, Mitsiades C, Tai YT, Hamasaki M, Raje N, Hideshima H, Schreiner G, Nguyen AN, Navas T, Munshi NC, Richardson PG, Higgins LS and Anderson KC. p38 MAPK inhibition enhances PS-341 (bortezomib)-induced cytotoxicity against multiple myeloma cells. Oncogene 2004; 23: 8766.

[41] Ishitsuka K, Hideshima T, Neri P, Vallet S, Shiraishi N, Okawa Y, Shen Z, Raje N, Kiziltepe T, Ocio EM, Chauhan D, Tassone P, Munshi N, Campbell RM, Dios AD, Shih C, Starling JJ, Tamura K and Anderson KC. p38 mitogen-activated protein kinase inhibitor LY2228820 enhances bortezomib-induced cytotoxicity and inhibits osteoclastogenesis in multiple myeloma; therapeutic implications. Br J Haematol 2008; 141: 598-606.

[42] Tate CM, Blosser W, Wyss L, Evans G, Xue Q, Pan Y and Stancato L. LY2228820 dimesylate, a selective inhibitor of p38 mitogen-activated protein kinase, reduces angiogenic endothelial cord formation in vitro and in vivo. J Biol Chem 2013; 288: 6743-53.